Published in final edited form as:

Structure. 2017 January 03; 25(1): 180–187. doi:10.1016/j.str.2016.11.007.

Structural Basis of Alcohol Inhibition of the Pentameric Ligand-gated Ion Channel ELIC

Qiang Chen[1], **Marta M. Wells**[1,4], **Tommy S. Tillman**[1], **Monica N. Kinde**[1], **Aina Cohen**[5], **Yan Xu**[1,2,3], and **Pei Tang**[1,2,4]

Qiang Chen: qic8@pitt.edu; Marta M. Wells: mmw88@pitt.edu; Tommy S. Tillman: tillman@pitt.edu; Monica N. Kinde: mkinde@kcumb.edu; Aina Cohen: acohen@slac.stanford.edu; Yan Xu: xuy@anes.upmc.edu

[1]Department of Anesthesiology, University of Pittsburgh School of Medicine

[2]Department of Pharmacology and Chemical Biology, University of Pittsburgh

[3]Department of Structural Biology, University of Pittsburgh

[4]Department of Computational and System Biology, University of Pittsburgh

[5]Stanford Synchrotron Radiation Lightsource

SUMMARY

The structural basis for alcohol modulation of neuronal pentameric ligand-gated ion channels (pLGICs) remains elusive. We determined an inhibitory mechanism of alcohol on the pLGIC *Erwinia chrysanthemi* (ELIC) through direct binding to the pore. X-ray structures of ELIC co-crystallized with 2-bromoethanol, in both the absence and presence of agonist, reveal 2-bromoethanol binding in the pore near T237(6′) and the extracellular domain (ECD) of each subunit at three different locations. Binding to the ECD does not appear to contribute to the inhibitory action of 2-bromoethanol and ethanol as indicated by the same functional responses of wild-type ELIC and mutants. In contrast, the ELIC-α1β3GABA$_A$R chimera, replacing the ELIC transmembrane domain (TMD) with the TMD of α1β3GABA$_A$R, is potentiated by 2-bromoethanol and ethanol. The results suggest a dominant role of the TMD in modulating alcohol effects. The X-ray structures and functional measurements support a pore-blocking mechanism for inhibitory action of short chain alcohols.

*Correspondence and lead contact: Pei Tang: ptang@pitt.edu.

ACCESSION NUMBERS

Crystal structures of BrEtOH-bound ELIC with (5SXU) and without (5SXV) PPA are deposited in the PDB.

SUPPLEMENTAL INFORMATION

Figs. S1–3, Table S1, and experimental details.

AUTHOR CONTRIBUTIONS

QC conducted most of the experiments and analyzed the results. TST and MMW performed TEVC measurements and participated in manuscript preparation. MNK expressed and prepared ELIC mutants for functional studies. AC along with QC contributed to X-ray data collection. YX and PT designed the project. PT and QC wrote the manuscript. All authors reviewed the results and approved the final version of the manuscript.

The authors declare no conflicts of interest with the contents of this article.

eTOC Blurb

Using X-ray crystallography and functional measurements, Chen et al. provide a structural basis for the pore-blocking mechanism for alcohol inhibition of ELIC, a pentameric ligand-gated ion channel.

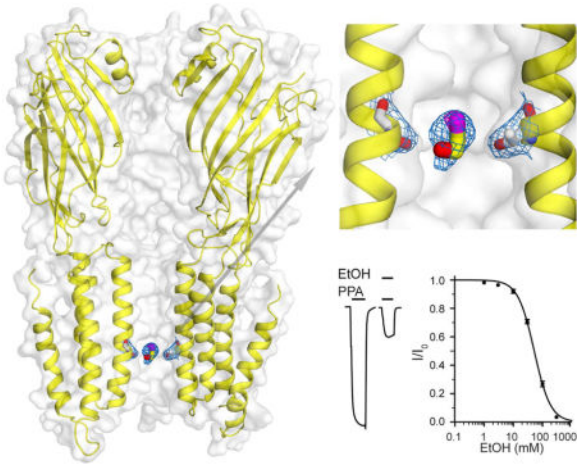

Keywords

alcohols; ethanol; pore blocking; ELIC; pentameric ligand-gated ion channels

INTRODUCTION

Chronic and acute effects of alcohol abuse cause huge health and economic burdens. The development of effective interventions and therapeutic options for alcohol abuse requires understanding the molecular mechanisms of alcohol action in the central nervous system (CNS). The complexity of alcohol action, however, has presented a great challenge for mechanistic investigation. Alcohols act on various proteins by different mechanisms (Deitrich et al., 1989; Forstera et al., 2016). Pentameric ligandgated ion channels (pLGICs) in the CNS, which include the inhibitory glycine receptors (GlyRs) and γ-aminobutyric acid type A receptors ($GABA_AR$s), and the excitatory serotonin receptors ($5HT_3$Rs) and nicotinic acetylcholine receptors (nAChRs), are plausible molecular targets of linear alcohols (*n*-alcohols). *n*-Alcohols enhance functions of GlyRs (Mascia et al., 1996a; Perkins et al., 2010) and most $GABA_AR$s (Mihic et al., 1997; Nakahiro et al., 1996), but suppress others such as α7nAChR and ρ1$GABA_AR$ (Cardoso et al., 1999; Covernton and Connolly, 1997; Mihic and Harris, 1996; Oz et al., 2005; Yu et al., 1996). Functional enhancement or suppression may depend on the molecular volume of alcohols and the receptor binding sites (Bradley et al., 1984; Cardoso et al., 1999; Nagata et al., 1996; Rusch et al., 2007; Stevens et al., 2005a; Stevens et al., 2005b; Wick et al., 1998). The phenomenon of alcohol cutoff (Pringle et al., 1981) has been observed for loss of righting reflex in tadpoles (Alifimoff et al., 1989) and also been observed in functional modulation of pLGICs (Dildy-Mayfield et al., 1996; Mascia et al., 1996a; Wick et al., 1998; Zuo et al., 2001). *N*-alcohols show an increase in potency with carbon chain length up until reaching a “cutoff” point, after which alcohol

potency declines or no longer increases with the increase of molecular size (Alifimoff et al., 1989; Wick et al., 1998). Different pLGICs may have different cutoff points, but mostly occur at n ≥ 10 (Dildy-Mayfield et al., 1996; Mascia et al., 1996a; Wick et al., 1998; Zuo et al., 2001). The cutoff phenomena support the presence of defined alcohol-binding sites.

Discrete alcohol-binding sites have been postulated in all three domains of pLGICs, including the extracellular (ECD), transmembrane (TMD), and intracellular (ICD) domains. Specific regions in the ECD, such as loop 2 of GlyRs and $GABA_A$Rs (Crawford et al., 2007; Mascia et al., 1996b; Perkins et al., 2012; Perkins et al., 2009) or loop D of β3-containing $GABA_A$Rs (Wallner et al., 2014), were identified to be responsible for ethanol sensitivity. Intracellular residues of GlyRs were found to be involved in mediating ethanol effects through altering interactions with G$\beta\gamma$ proteins (Qi et al., 2007; Yevenes et al., 2010; Yevenes et al., 2008). For the TMD, mutagenesis and labeling studies suggested alcohol allosteric modulation sites outside the pore in α1GlyR (Mascia et al., 2000; Mihic et al., 1997; Wick et al., 1998; Yamakura et al., 1999; Ye et al., 1998), $GABA_A$Rs (Jung et al., 2005; Mascia et al., 2000; Mihic et al., 1997; Wick et al., 1998), and $5HT3_A$Rs (Hu et al., 2006). In addition, alcohol binding to the pore residues of nAChRs was documented based on mutagenesis, photolabeling, and functional measurements (Borghese et al., 2003b; Forman et al., 1995; Forman and Zhou, 2000; Forman et al., 2007; Pratt et al., 2000; Zhou et al., 2000).

In contrast to the abundant data from mutagenesis and functional measurements, high-resolution structures of pLGICs showing alcohol binding are scarce (Sauguet et al., 2013). In this study, we investigated alcohol modulation of ELIC, a prokaryotic pLGIC from *Erwinia chrysanthemi*, and found inhibitory effects of alcohols on ELIC similar to those observed on α7nAChR (Cardoso et al., 1999; Oz et al., 2005; Yu et al., 1996) and ρ1$GABA_A$R (Mihic and Harris, 1996; Wick et al., 1998). X-ray structures of ELIC co-crystallized with 2-bromoethanol (BrEtOH) under resting and desensitized conditions reveal BrEtOH binding to the pore and to three sites within the ECD for each subunit. Electrophysiological measurements of ELIC mutants and an ELIC-α1β3$GABA_A$R chimera define a determinant role of alcohol binding inside the pore for the functional inhibition of ELIC. The study provides compelling evidence to support an inhibitory mechanism of alcohol through a direct binding to the pore of pLGICs.

RESULTS

Concentration dependence and cutoff phenomenon of alcohol inhibition of ELIC

The current elicited by the agonist propylamine (PPA) in *Xenopus* oocytes expressing ELIC was inhibited in a concentration-dependent manner by ethanol (EtOH) and other *n*-alcohols up to *n*-nonanol (Fig. 1 and Table S1), showing a positive association between the inhibitory potency and the alkyl chain length of these *n*-alcohols. The longer chain alcohols *n*-decanol and *n*-dodecanol, however, do not fit the association. Even at their respective highest soluble concentrations, *n*-decanol (~0.3 mM) produces much weaker inhibition than *n*-nonanol or *n*-hexanol, while *n*-dodecanol (~0.02 mM) shows no sign of inhibition of ELIC (Fig. 1b). This cutoff phenomenon has been observed on other pLGICs (Dildy-Mayfield et al., 1996; Mascia et al., 1996a; Zuo et al., 2001). BrEtOH, an EtOH analog, also inhibited ELIC with a

higher potency (Fig. 1b and Table S1), which may result from a slightly larger molecular size and greater hydrophobicity of BrEtOH than EtOH (Table S1).

Multiple alcohol-binding sites in ELIC

We co-crystalized ELIC with BrEtOH, rather than EtOH, because the anomalous signal from bromine in BrEtOH is essential to determine binding sites for small molecules with low binding affinities, such as EtOH (Sauguet et al., 2013). X-ray structures show well-defined anomalous signals from BrEtOH and structural resolutions up to 3.1 Å and 3.4 Å in the presence and absence of the agonist PPA, corresponding to the desensitized and resting conditions of ELIC, respectively. Table 1 summarizes crystallographic and refinement parameters. The overlay of the strong Br-specific anomalous difference density maps onto the F_O-F_C omitted electron density maps show three sets of BrEtOH binding sites in the ECD (Figs. 2a, b) and one inside the pore near residue T237(6′) (Fig. 2c) in both the resting (Fig. 2a) and desensitized (Fig. 2b) conditions. The $2F_O$-F_C electron density maps show the refined structures of BrEtOH molecules bound in the ECD (Figs. 2d, 2e) and inside the pore (Fig. 2f) of ELIC. Note that T237(6′) is a highly conserved residue at the 6′ pore position of pLGICs (Fig. S1). All three BrEtOH sites in the ECD belong to intra-subunit binding pockets. Two are located between loop A and loop E (Fig. 2d), and the third is between loop G (also called loop 2) and loop F (Fig. 2e). In addition to Van der Waals' interactions, hydrogen bonding is also involved in BrEtOH interactions with nearby residues, including P74 and A75 of loop A, Y102 of loop E, I20 of loop G, and T237(6′) of TM2 (Fig. 3). Contribution of hydrogen bonds to alcohol binding was also observed in previous crystallographic studies (Olsen et al., 2014; Sauguet et al., 2013; Thode et al., 2008).

Structural comparison with apo ELIC (PDB code: 3RQU) (Pan et al., 2012b) revealed an inward movement of loop C in the BrEtOH-bound ELIC in the presence of the agonist PPA (PDB code: 5SXU). The maximum displacement of loop C is ~1.5 Å, measured by Cα distances in the aligned structures (Fig. S2). The agonist binding is most likely responsible for the loop C displacement because the BrEtOH-bound ELIC in the absence of agonist (PDB code: 5SXV) did not show such a change (Fig. S2). There is no obvious structural change in the ECD attributed to BrEtOH binding. In the TMD, small reductions of pore radius (~0.5 Å or less) near 16′ and 6′ residue positions were observed in the BrEtOH-bound ELIC with PPA (Fig. S3). Without PPA, the pore radius had negligible change upon BrEtOH binding (Fig. S3). Overall, there is no significant change induced by BrEtOH binding.

Alcohol binding to the pore dominates functional inhibition of ELIC

Among the multiple binding sites revealed in the crystal structures, are all of them involved in functional modulation? Which site is primarily responsible for inhibition of ELIC? To answer these questions, we made mutations to residues whose side chains contact BrEtOH: I23C and Y102F in the ECD and T237(6′)A in the TMD. The functional measurements showed that the mutations in the ECD yielded minimal impact to EtOH and BrEtOH modulation of ELIC (Figs. 4a, b). In addition, changing the molecular volume by tagging I23C with 4-(chloromercuri)benzenesulfonic acid (pCMBS) also did not affect EtOH and BrEtOH modulation (Figs. 4a, b). In contrast, the TMD T237(6′)A mutation inside the pore

significantly weakened inhibition by EtOH and BrEtOH (Fig. 4c). The higher inhibitory potency of BrEtOH over EtOH may mostly result from the ~10% greater molecular radius of BrEtOH, which provides better contact with pore residues. The mutation T237(6′)A increases the pore radius by ~10% (Zamyatnin, 1972), thereby eliminating the optimal contacts of BrEtOH to pore residues and shifting the inhibitory potency of BrEtOH to be closer to that of EtOH. EtOH, on the other hand, has suboptimal contacts in the first place. Therefore, the potency reduction of EtOH in the T237(6′)A mutant is less profound.

To further establish the role of alcohol binding to the pore in functional inhibition of ELIC, we measured alcohol modulation of ELIC-α1β3GABA$_A$R, a chimera that has the ECD of ELIC and the TMD of α1β3GABA$_A$R (Kinde et al., 2016). Distinctly different from the inhibitory effect on ELIC, but similar to the potentiating effect on α1β3GABA$_A$R, EtOH and BrEtOH potentiate ELIC-α1β3GABA$_A$R substantially at low agonist concentration (EC_3) (Fig. 4d). At higher agonist concentration (EC_{20}), EtOH and BrEtOH still fully inhibit ELIC, but at the same concentrations neither EtOH nor BrEtOH inhibits ELIC-α1β3GABA$_A$R. In fact, BrEtOH potentiates ELIC-α1β3GABA$_A$R, even at higher agonist concentrations (Fig. 4e). Clearly, the ELIC-α1β3GABA$_A$R chimera resembles α1β3GABA$_A$R in its functional potentiation by these alcohols, not the inhibitory response of ELIC. The insensitive inhibitory responses to mutations and the pCMBS labeling in the ECD set a contrast with the sensitive response to the TMD mutation and functional potentiation of the ELIC-α1β3GABA$_A$R chimera by EtOH and BrEtOH. The results suggest that BrEtOH as well as EtOH binding to the pore dominates functional inhibition of ELIC.

DISCUSSION

Accurate determination of EtOH binding sites has proven difficult in the past due to the small molecular size of EtOH and its low affinity to pLGICs (Sauguet et al., 2013). Anomalous signals from BrEtOH enabled an unambiguous identification of binding sites in the X-ray structures of ELIC. A previous crystallographic study of GLIC demonstrated that all of the BrEtOH binding sites also bind EtOH (Sauguet et al., 2013). Our functional measurements showed consistent parallel responses of ELIC, ELIC mutants, and ELIC-α1β3GABA$_A$R to both EtOH and BrEtOH. Thus, there is a high likelihood that EtOH binds to the same BrEtOH sites as shown in ELIC crystal structures.

Our combined structural and functional data support a direct pore-blocking mechanism for alcohol inhibition. BrEtOH occupies the 6′ position of the pore in both the resting and desensitized states. Interestingly, the recent crystallographic and functional investigations of isoflurane action on ELIC (Chen et al., 2015) show that isoflurane also inhibits ELIC through binding to the pore at two different sites, comprised of residues at the 6′ and 13′ positions (Chen et al., 2015). These crystal structures suggest that alcohols and anesthetics may inhibit ELIC through the same pore-blocking mechanism (Chen et al., 2015).

The pore-blocking mechanism for inhibitory action of long- and short-chain alcohols has been proposed for nAChRs (Borghese et al., 2003b; Forman et al., 1995; Forman and Zhou, 2000; Forman et al., 2007; Pratt et al., 2000; Zhou et al., 2000). At physiological concentrations, *n*-alcohols from propanol through decanol inhibit muscle nAChRs (Forman

and Miller, 1989). Ethanol does not inhibit wild-type muscle nAChRs, but hydrophobic mutations in the 10′ position of the pore greatly increased sensitivity to ethanol inhibition (Forman and Zhou, 2000). Photolabeling of 3-azioctanol to *Torpedo* nAChRs identified a major binding site in the 20′ position at the extracellular end of the pore (Pratt et al., 2000). Different *n*-alcohols may interact with different portions of the pore. The shorter chain EtOH was predicted to bind more deeply within the pore (Zhou et al., 2000). A recent mutagenesis study on ρ1GABA$_A$R suggested an inhibitory binding site of EtOH at the 6′ position in the pore (Borghese et al., 2016). Our structural and functional studies support a mechanism of alcohol inhibition through binding within the pore and provide atomic structures of BrEtOH binding to the 6′ position of ELIC.

It has been suggested that alcohol action may involve binding to multiple sites, with some sites even leading to opposing functional consequences (Borghese et al., 2003a; Howard et al., 2011). Our crystal structures reveal several BrEtOH-binding sites in the ECD in addition to the 6′ position in the pore, but we did not observe any opposing functional effects from the ECD sites in ELIC. If the ECD sites were involved in potentiation, mutation of these sites should reduce the potentiation effects and give a net gain of alcohol inhibition. The fact that the mutations did not alter alcohol modulation suggests that the ECD sites have no functional impact. We conclude that not every binding site has functional impact. The same conclusion was also obtained from our previous study of propofol binding and modulation of ELIC (Kinde et al., 2016).

In the case of BrEtOH binding, we did not and probably should not expect to observe profound structural changes. BrEtOH generates inhibitory effects and should promote a closed structure, like the structure of apo ELIC, even in the presence of agonist. Insensitive structural responses to binding of small ligand molecules were also observed previously in ELIC and other pLGICs (Chen et al., 2015; Hibbs and Gouaux, 2011; Nury et al., 2011; Pan et al., 2012a; Sauguet et al., 2013), presumably due to low affinities of binding molecules and crystallization conditions that damped intrinsic structural flexibility accompanying functional changes upon binding of small molecules, such as BrEtOH.

Pore blocking is the dominant mechanism in EtOH inhibition of ELIC, but may not necessarily be a dominant mechanism for inhibitory modulations by other alcohols and anesthetics. For example, propofol was found to inhibit ELIC through a common TMD intra-subunit binding pocket (Kinde et al., 2016), which is shared by several anesthetics in GLIC and nAChR (Chiara et al., 2003; Chiara et al., 2014; Chiara et al., 2009; Hamouda et al., 2011; Jayakar et al., 2013; Nury et al., 2011).

EtOH binding to the ECD does not yield measureable impact to the function of ELIC, but may produce functional consequences in other pLGICs. An early study using the α7nAChR-5HT$_3$R chimera suggested that EtOH binding to the ECD of α7nAChR was responsible for α7nAChR inhibition (Yu et al., 1996). Interestingly, sequence alignment (Fig. S1) shows that ELIC and α7nAChR as well as ρ1GABA$_A$R are likely to have the same binding sites for ethanol because they share homologous or identical residues in the binding sites shown in the ELIC crystal structures (Fig. 2). Of course, the size of each pocket affects alcohol binding and subsequent functional consequences. Unfortunately, neither α7nAChR

nor ρ1GABA$_A$R presently have crystal structures to allow for comparisons with ELIC. The study reported here provides a valuable structural basis for the dissection of alcohol inhibition of pLGICs with atomic resolutions.

EXPERIMENTAL PROCEDURES

ELIC was expressed, purified, and crystallized as reported previously (Chen et al., 2015; Kinde et al., 2015; Pan et al., 2012b). ELIC was concentrated to 5 ~ 6 mg/ml for crystallization after BrEtOH (100 mM) or PPA (5 mM) was mixed with ELIC for at least 30 minutes. Crystallization was at 4°C using the sitting-drop plate (Hampton Research). All chemicals were purchased from Sigma-Aldrich (St. Louis, MO).

Crystals were harvested in liquid nitrogen after cryo-protection with up to 20% glycerol. The X-ray diffraction data were collected on beamline 12–2 at the Stanford Synchrotron Radiation Lightsource (SSRL). The data were indexed, integrated, and scaled with the XDS program (Kabsch, 2010). The published ELIC structure (PDB code: 3RQU) was used for the structure determination of BrEtOH-bound ELIC. The binding sites of BrEtOH were determined based on the bromine-specific (0.9195 Å) anomalous difference map. Torsional non-crystallographic symmetry (NCS) restraints were applied to all subunits in the asymmetric unit. The final structures were analyzed using Phenix (Adams et al., 2010) and MolProbility (Davis et al., 2004), and the graphics were prepared using PyMol (DeLano, 2002).

Functional measurements of *Xenopus laevis* oocytes expressing ELIC, its mutants, and the ELIC-GABA$_A$R chimeras and the data analysis were performed as reported previously (Kinde et al., 2016; Kinde et al., 2015; Pan et al., 2012a; Pan et al., 2012b; Tillman et al., 2013; Tillman et al., 2014; Wells et al., 2015). All the procedures involving *Xenopus laevis* oocytes were approved by the University of Pittsburgh Institutional Animal Care and Use Committee.

Supplementary Material

Refer to Web version on PubMed Central for supplementary material.

Acknowledgments

The authors thank Dr. Palaniappa Arjunan for his help in the structure refinements. Use of the Stanford Synchrotron Radiation Lightsource, SLAC National Accelerator Laboratory, is supported by the U.S. Department of Energy, Office of Science, Office of Basic Energy Sciences under Contract No. DE-AC02-76SF00515, the National Institutes of Health, and National Institute of General Medical Sciences (including P41GM103393). The research was supported by NIH (R01GM056257 and R01GM066358).

References

Adams PD, Afonine PV, Bunkoczi G, Chen VB, Davis IW, Echols N, Headd JJ, Hung LW, Kapral GJ, Grosse-Kunstleve RW, et al. PHENIX: a comprehensive Python-based system for macromolecular structure solution. Acta Crystallogr D Biol Crystallogr. 2010; 66:213–221. [PubMed: 20124702]

Alifimoff JK, Firestone LL, Miller KW. Anaesthetic potencies of primary alkanols: implications for the molecular dimensions of the anaesthetic site. Br J Pharmacol. 1989; 96:9–16. [PubMed: 2784337]

Borghese CM, Henderson LA, Bleck V, Trudell JR, Harris RA. Sites of excitatory and inhibitory actions of alcohols on neuronal alpha2beta4 nicotinic acetylcholine receptors. J Pharmacol Exp Ther. 2003a; 307:42–52. [PubMed: 14500778]

Borghese CM, Ruiz CI, Lee US, Cullins MA, Bertaccini EJ, Trudell JR, Harris RA. Identification of an Inhibitory Alcohol Binding Site in GABAA rho1 Receptors. ACS Chem Neurosci. 2016; 7:100–108. [PubMed: 26571107]

Borghese CM, Wang L, Bleck V, Harris RA. Mutation in neuronal nicotinic acetylcholine receptors expressed in Xenopus oocytes blocks ethanol action. Addict Biol. 2003b; 8:313–318. [PubMed: 13129833]

Bradley RJ, Sterz R, Peper K. The effects of alcohols and diols at the nicotinic acetylcholine receptor of the neuromuscular junction. Brain Res. 1984; 295:101–112. [PubMed: 6608971]

Cardoso RA, Brozowski SJ, Chavez-Noriega LE, Harpold M, Valenzuela CF, Harris RA. Effects of ethanol on recombinant human neuronal nicotinic acetylcholine receptors expressed in Xenopus oocytes. J Pharmacol Exp Ther. 1999; 289:774–780. [PubMed: 10215652]

Chen Q, Kinde MN, Arjunan P, Wells MM, Cohen AE, Xu Y, Tang P. Direct Pore Binding as a Mechanism for Isoflurane Inhibition of the Pentameric Ligand-gated Ion Channel ELIC. Sci Rep. 2015; 5:13833. [PubMed: 26346220]

Chiara DC, Dangott LJ, Eckenhoff RG, Cohen JB. Identification of nicotinic acetylcholine receptor amino acids photolabeled by the volatile anesthetic halothane. Biochemistry. 2003; 42:13457–13467. [PubMed: 14621991]

Chiara DC, Gill JF, Chen Q, Tillman T, Dailey WP, Eckenhoff RG, Xu Y, Tang P, Cohen JB. Photoaffinity labeling the propofol binding site in GLIC. Biochemistry. 2014; 53:135–142. [PubMed: 24341978]

Chiara DC, Hamouda AK, Ziebell MR, Mejia LA, Garcia G 3rd, Cohen JB. [(3)H]chlorpromazine photolabeling of the torpedo nicotinic acetylcholine receptor identifies two state-dependent binding sites in the ion channel. Biochemistry. 2009; 48:10066–10077. [PubMed: 19754159]

Covernton PJ, Connolly JG. Differential modulation of rat neuronal nicotinic receptor subtypes by acute application of ethanol. Br J Pharmacol. 1997; 122:1661–1668. [PubMed: 9422812]

Crawford DK, Trudell JR, Bertaccini EJ, Li K, Davies DL, Alkana RL. Evidence that ethanol acts on a target in Loop 2 of the extracellular domain of alpha1 glycine receptors. J Neurochem. 2007; 102:2097–2109. [PubMed: 17561937]

Davis IW, Murray LW, Richardson JS, Richardson DC. MOLPROBITY: structure validation and all-atom contact analysis for nucleic acids and their complexes. Nucleic Acids Res. 2004; 32:W615–619. [PubMed: 15215462]

Deitrich RA, Dunwiddie TV, Harris RA, Erwin VG. Mechanism of action of ethanol: initial central nervous system actions. Pharmacol Rev. 1989; 41:489–537. [PubMed: 2700603]

DeLano, WL. The PyMOL Molecular Graphics System. Schrödinger, LLC; Palo Alto, CA, Delano Scientific LLC: 2002.

Dildy-Mayfield JE, Mihic SJ, Liu Y, Deitrich RA, Harris RA. Actions of long chain alcohols on GABAA and glutamate receptors: relation to in vivo effects. Br J Pharmacol. 1996; 118:378–384. [PubMed: 8735641]

Forman SA, Miller KW. Molecular sites of anesthetic action in postsynaptic nicotinic membranes. Trends Pharmacol Sci. 1989; 10:447–452. [PubMed: 2692257]

Forman SA, Miller KW, Yellen G. A discrete site for general anesthetics on a postsynaptic receptor. Mol Pharmacol. 1995; 48:574–581. [PubMed: 7476881]

Forman SA, Zhou Q. Nicotinic receptor pore mutations create a sensitive inhibitory site for ethanol. Alcohol Clin Exp Res. 2000; 24:1363–1368. [PubMed: 11003201]

Forman SA, Zhou QL, Stewart DS. Photoactivated 3-azioctanol irreversibly desensitizes muscle nicotinic ACh receptors via interactions at alphaE262. Biochemistry. 2007; 46:11911–11918. [PubMed: 17910479]

Forstera B, Castro PA, Moraga-Cid G, Aguayo LG. Potentiation of Gamma Aminobutyric Acid Receptors (GABAAR) by Ethanol: How Are Inhibitory Receptors Affected? Front Cell Neurosci. 2016; 10:114. [PubMed: 27199667]

Hamouda AK, Stewart DS, Husain SS, Cohen JB. Multiple transmembrane binding sites for p-trifluoromethyldiazirinyl-etomidate, a photoreactive Torpedo nicotinic acetylcholine receptor allosteric inhibitor. J Biol Chem. 2011; 286:20466–20477. [PubMed: 21498509]

Hibbs RE, Gouaux E. Principles of activation and permeation in an anion-selective Cys-loop receptor. Nature. 2011; 474:54–60. [PubMed: 21572436]

Howard RJ, Slesinger PA, Davies DL, Das J, Trudell JR, Harris RA. Alcohol-binding sites in distinct brain proteins: the quest for atomic level resolution. Alcohol Clin Exp Res. 2011; 35:1561–1573. [PubMed: 21676006]

Hu XQ, Hayrapetyan V, Gadhiya JJ, Rhubottom HE, Lovinger DM, Machu TK. Mutations of L293 in transmembrane two of the mouse 5-hydroxytryptamine3A receptor alter gating and alcohol modulatory actions. Br J Pharmacol. 2006; 148:88–101. [PubMed: 16520747]

Jayakar SS, Dailey WP, Eckenhoff RG, Cohen JB. Identification of propofol binding sites in a nicotinic acetylcholine receptor with a photoreactive propofol analog. J Biol Chem. 2013; 288:6178–6189. [PubMed: 23300078]

Jung S, Akabas MH, Harris RA. Functional and structural analysis of the GABAA receptor alpha 1 subunit during channel gating and alcohol modulation. J Biol Chem. 2005; 280:308–316. [PubMed: 15522868]

Kabsch W. Xds. Acta Crystallogr D Biol Crystallogr. 2010; 66:125–132. [PubMed: 20124692]

Kinde MN, Bu W, Chen Q, Xu Y, Eckenhoff RG, Tang P. Common Anesthetic-binding Site for Inhibition of Pentameric Ligand-gated Ion Channels. Anesthesiology. 2016; 124:664–673. [PubMed: 26756520]

Kinde MN, Chen Q, Lawless MJ, Mowrey DD, Xu J, Saxena S, Xu Y, Tang P. Conformational Changes Underlying Desensitization of the Pentameric Ligand-Gated Ion Channel ELIC. Structure. 2015; 23:995–1004. [PubMed: 25960405]

Mascia MP, Machu TK, Harris RA. Enhancement of homomeric glycine receptor function by long-chain alcohols and anaesthetics. Br J Pharmacol. 1996a; 119:1331–1336. [PubMed: 8968539]

Mascia MP, Mihic SJ, Valenzuela CF, Schofield PR, Harris RA. A single amino acid determines differences in ethanol actions on strychnine-sensitive glycine receptors. Mol Pharmacol. 1996b; 50:402–406. [PubMed: 8700149]

Mascia MP, Trudell JR, Harris RA. Specific binding sites for alcohols and anesthetics on ligand-gated ion channels. Proc Natl Acad Sci U S A. 2000; 97:9305–9310. [PubMed: 10908659]

Mihic SJ, Harris RA. Inhibition of rho1 receptor GABAergic currents by alcohols and volatile anesthetics. J Pharmacol Exp Ther. 1996; 277:411–416. [PubMed: 8613949]

Mihic SJ, Ye Q, Wick MJ, Koltchine VV, Krasowski MD, Finn SE, Mascia MP, Valenzuela CF, Hanson KK, Greenblatt EP, et al. Sites of alcohol and volatile anaesthetic action on GABA(A) and glycine receptors. Nature. 1997; 389:385–389. [PubMed: 9311780]

Nagata K, Aistrup GL, Huang CS, Marszalec W, Song JH, Yeh JZ, Narahashi T. Potent modulation of neuronal nicotinic acetylcholine receptor-channel by ethanol. Neurosci Lett. 1996; 217:189–193. [PubMed: 8916104]

Nakahiro M, Arakawa O, Nishimura T, Narahashi T. Potentiation of GABA-induced Cl- current by a series of n-alcohols disappears at a cutoff point of a longer-chain n-alcohol in rat dorsal root ganglion neurons. Neurosci Lett. 1996; 205:127–130. [PubMed: 8907333]

Nury H, Van Renterghem C, Weng Y, Tran A, Baaden M, Dufresne V, Changeux JP, Sonner JM, Delarue M, Corringer PJ. X-ray structures of general anaesthetics bound to a pentameric ligand-gated ion channel. Nature. 2011; 469:428–431. [PubMed: 21248852]

Olsen RW, Li GD, Wallner M, Trudell JR, Bertaccini EJ, Lindahl E, Miller KW, Alkana RL, Davies DL. Structural models of ligand-gated ion channels: sites of action for anesthetics and ethanol. Alcohol Clin Exp Res. 2014; 38:595–603. [PubMed: 24164436]

Oz M, Jackson SN, Woods AS, Morales M, Zhang L. Additive effects of endogenous cannabinoid anandamide and ethanol on alpha7-nicotinic acetylcholine receptor-mediated responses in Xenopus Oocytes. J Pharmacol Exp Ther. 2005; 313:1272–1280. [PubMed: 15687372]

Pan J, Chen Q, Willenbring D, Mowrey D, Kong XP, Cohen A, Divito CB, Xu Y, Tang P. Structure of the pentameric ligand-gated ion channel GLIC bound with anesthetic ketamine. Structure. 2012a; 20:1463–1469. [PubMed: 22958642]

Pan J, Chen Q, Willenbring D, Yoshida K, Tillman T, Kashlan OB, Cohen A, Kong XP, Xu Y, Tang P. Structure of the pentameric ligand-gated ion channel ELIC cocrystallized with its competitive antagonist acetylcholine. Nat Commun. 2012b; 3:714. [PubMed: 22395605]

Perkins DI, Trudell JR, Asatryan L, Davies DL, Alkana RL. Charge and geometry of residues in the loop 2 beta hairpin differentially affect agonist and ethanol sensitivity in glycine receptors. J Pharmacol Exp Ther. 2012; 341:543–551. [PubMed: 22357974]

Perkins DI, Trudell JR, Crawford DK, Alkana RL, Davies DL. Molecular targets and mechanisms for ethanol action in glycine receptors. Pharmacol Ther. 2010; 127:53–65. [PubMed: 20399807]

Perkins DI, Trudell JR, Crawford DK, Asatryan L, Alkana RL, Davies DL. Loop 2 structure in glycine and GABA(A) receptors plays a key role in determining ethanol sensitivity. J Biol Chem. 2009; 284:27304–27314. [PubMed: 19656948]

Pratt MB, Husain SS, Miller KW, Cohen JB. Identification of sites of incorporation in the nicotinic acetylcholine receptor of a photoactivatible general anesthetic. J Biol Chem. 2000; 275:29441–29451. [PubMed: 10859324]

Pringle MJ, Brown KB, Miller KW. Can the lipid theories of anesthesia account for the cutoff in anesthetic potency in homologous series of alcohols? Mol Pharmacol. 1981; 19:49–55. [PubMed: 7207463]

Qi ZH, Song M, Wallace MJ, Wang D, Newton PM, McMahon T, Chou WH, Zhang C, Shokat KM, Messing RO. Protein kinase C epsilon regulates gamma-aminobutyrate type A receptor sensitivity to ethanol and benzodiazepines through phosphorylation of gamma2 subunits. J Biol Chem. 2007; 282:33052–33063. [PubMed: 17875639]

Rusch D, Musset B, Wulf H, Schuster A, Raines DE. Subunit-dependent modulation of the 5-hydroxytryptamine type 3 receptor open-close equilibrium by n-alcohols. J Pharmacol Exp Ther. 2007; 321:1069–1074. [PubMed: 17360702]

Sauguet L, Howard RJ, Malherbe L, Lee US, Corringer PJ, Harris RA, Delarue M. Structural basis for potentiation by alcohols and anaesthetics in a ligand-gated ion channel. Nat Commun. 2013; 4:1697. [PubMed: 23591864]

Stevens R, Rusch D, Solt K, Raines DE, Davies PA. Modulation of human 5-hydroxytryptamine type 3AB receptors by volatile anesthetics and n-alcohols. J Pharmacol Exp Ther. 2005a; 314:338–345. [PubMed: 15831437]

Stevens RJ, Rusch D, Davies PA, Raines DE. Molecular properties important for inhaled anesthetic action on human 5-HT3A receptors. Anesth Analg. 2005b; 100:1696–1703. [PubMed: 15920198]

Thode AB, Kruse SW, Nix JC, Jones DN. The role of multiple hydrogen-bonding groups in specific alcohol binding sites in proteins: insights from structural studies of LUSH. J Mol Biol. 2008; 376:1360–1376. [PubMed: 18234222]

Tillman T, Cheng MH, Chen Q, Tang P, Xu Y. Reversal of ion-charge selectivity renders the pentameric ligand-gated ion channel GLIC insensitive to anaesthetics. Biochem J. 2013; 449:61–68. [PubMed: 22978431]

Tillman TS, Seyoum E, Mowrey DD, Xu Y, Tang P. ELIC-alpha7 Nicotinic acetylcholine receptor (alpha7nAChR) chimeras reveal a prominent role of the extracellular-transmembrane domain interface in allosteric modulation. J Biol Chem. 2014; 289:13851–13857. [PubMed: 24695730]

Wallner M, Hanchar HJ, Olsen RW. Alcohol selectivity of beta3-containing GABAA receptors: evidence for a unique extracellular alcohol/imidazobenzodiazepine Ro15-4513 binding site at the alpha+beta− subunit interface in alphabeta3delta GABAA receptors. Neurochem Res. 2014; 39:1118–1126. [PubMed: 24500446]

Wells MM, Tillman TS, Mowrey DD, Sun T, Xu Y, Tang P. Ensemble-based virtual screening for cannabinoid-like potentiators of the human glycine receptor alpha1 for the treatment of pain. J Med Chem. 2015; 58:2958–2966. [PubMed: 25790278]

Wick MJ, Mihic SJ, Ueno S, Mascia MP, Trudell JR, Brozowski SJ, Ye Q, Harrison NL, Harris RA. Mutations of gamma-aminobutyric acid and glycine receptors change alcohol cutoff: evidence for an alcohol receptor? Proc Natl Acad Sci U S A. 1998; 95:6504–6509. [PubMed: 9600996]

Yamakura T, Mihic SJ, Harris RA. Amino acid volume and hydropathy of a transmembrane site determine glycine and anesthetic sensitivity of glycine receptors. J Biol Chem. 1999; 274:23006–23012. [PubMed: 10438467]

Ye Q, Koltchine VV, Mihic SJ, Mascia MP, Wick MJ, Finn SE, Harrison NL, Harris RA. Enhancement of glycine receptor function by ethanol is inversely correlated with molecular volume at position alpha267. J Biol Chem. 1998; 273:3314–3319. [PubMed: 9452448]

Yevenes GE, Moraga-Cid G, Avila A, Guzman L, Figueroa M, Peoples RW, Aguayo LG. Molecular requirements for ethanol differential allosteric modulation of glycine receptors based on selective Gbetagamma modulation. J Biol Chem. 2010; 285:30203–30213. [PubMed: 20647311]

Yevenes GE, Moraga-Cid G, Peoples RW, Schmalzing G, Aguayo LG. A selective G betagamma-linked intracellular mechanism for modulation of a ligand-gated ion channel by ethanol. Proc Natl Acad Sci U S A. 2008; 105:20523–20528. [PubMed: 19074265]

Yu D, Zhang L, Eisele JL, Bertrand D, Changeux JP, Weight FF. Ethanol inhibition of nicotinic acetylcholine type alpha 7 receptors involves the amino-terminal domain of the receptor. Mol Pharmacol. 1996; 50:1010–1016. [PubMed: 8863848]

Zamyatnin AA. Protein volume in solution. Prog Biophys Mol Biol. 1972; 24:107–123. [PubMed: 4566650]

Zhou QL, Zhou Q, Forman SA. The n-alcohol site in the nicotinic receptor pore is a hydrophobic patch. Biochemistry. 2000; 39:14920–14926. [PubMed: 11101308]

Zuo Y, Aistrup GL, Marszalec W, Gillespie A, Chavez-Noriega LE, Yeh JZ, Narahashi T. Dual action of n-alcohols on neuronal nicotinic acetylcholine receptors. Mol Pharmacol. 2001; 60:700–711. [PubMed: 11562431]

Highlights

- *n*-Alcohols, including 2-bromoethanol (BrEtOH), inhibit the function of ELIC.
- Crystal structures show BrEtOH binding sites in the pore and the ECD of ELIC.
- BrEtOH binding to the pore at the 6′ position dominates its inhibitory action.

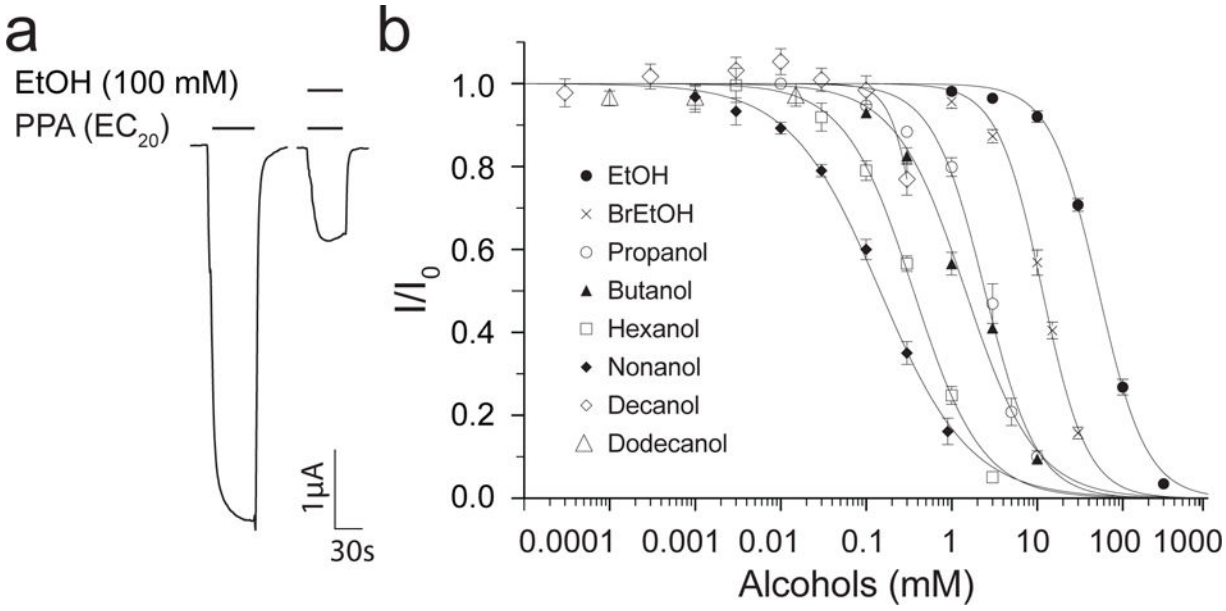

Figure 1. Inhibition of ELIC by *n*-alcohols

(**a**) Representative current traces of *Xenopus laevis* oocytes expressing ELIC, showing ethanol inhibition of the current elicited by the agonist propylamine (PPA). The horizontal and vertical scale bars represent 1 μA and 30 sec, respectively. (**b**) Concentration-dependent inhibition of ELIC by *n*-alcohols. All data were normalized to the current at EC_{20} in the absence of alcohols and fit to the Hill equation (solid lines, $n \geq 6$). The best-fit IC_{50} values for ethanol (•), 2-bromoethanol (×), *n*-propanol (○), *n*-butanol (▲), *n*-hexanol (□), and *n*-nonanol (◆) are reported in the main text as the mean ± SEM. Error bars less than the symbols sizes are not visible.

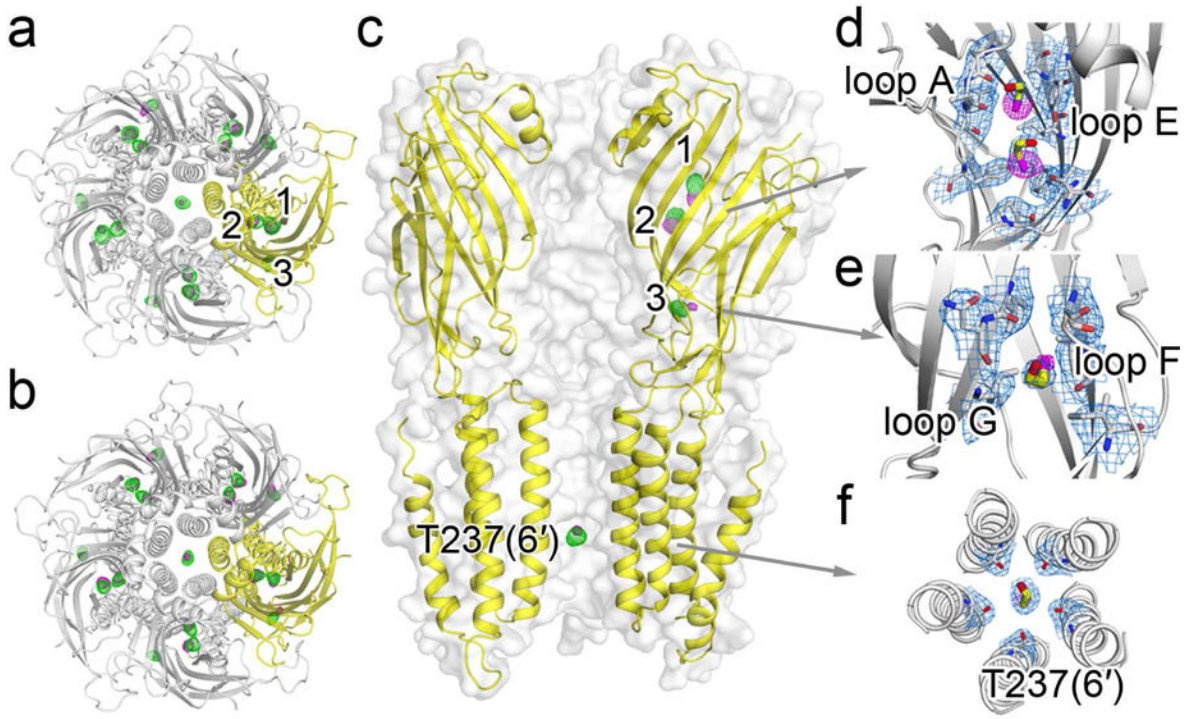

Figure 2. Crystal structures of ELIC showing 2-bromoethanol (BrEtOH) binding sites

Top views of BrEtOH binding to ELIC in (**a**) the resting and (**b**) desensitized states. (**c**) Side view of BrEtOH binding to ELIC in the desensitized state. The F_O-F_C omitted electron density maps (green) are contoured at 3.0 σ. The anomalous difference electron maps (magenta) are contoured at (a) 4.0 σ and (b) 5.0 σ for the resting and desensitized ELIC, respectively. (**d**)–(**f**) $2F_O$-F_C electron density maps (light blue, contoured at 1.0 σ) of ELIC in a desensitized state showing: (**d**) two BrEtOH molecules bound to a pocket in the ECD lined by loop A and loop E; (**e**) the third BrEtOH in the ECD bound to a pocket between loop G and loop F; and (**f**) a bottom view of BrEtOH bound to the pore near T237(6′). Residues within 4 Å of BrEtOH molecules are shown as sticks. The maps from (a) to (f) all have a carve distance of 2.0 Å from BrEtOH molecules.

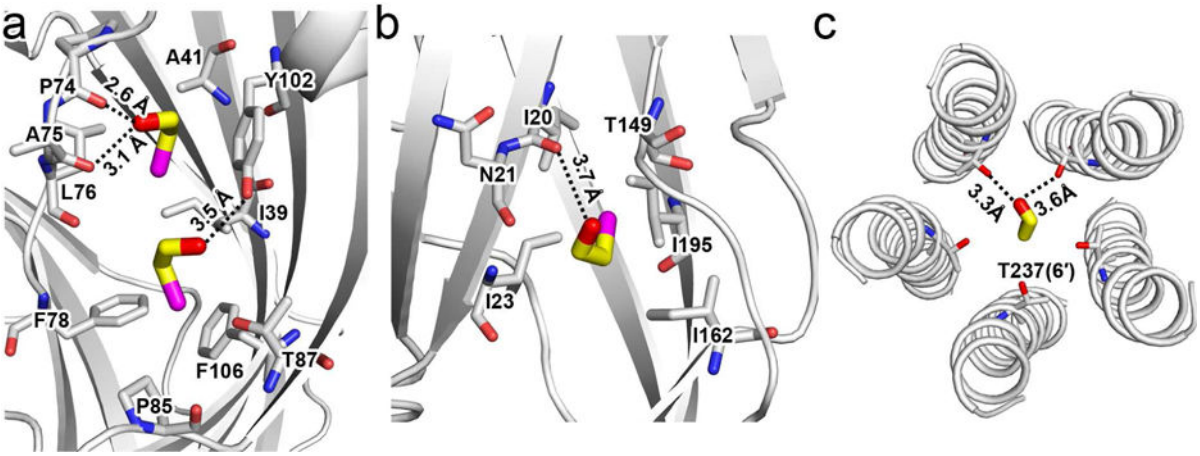

Figure 3. Molecular interactions between ELIC and 2-bromoethanol (BrEtOH)

(**a**) Two BrEtOH molecules in the ECD interact with the surrounding residues and form hydrogen bonds with the backbone carbonyl oxygen of P74 and A75, and the hydroxyl group of Y102. (**b**) BrEtOH in the ECD forms a hydrogen bond with the carbonyl oxygen of I20. (**c**) BrEtOH in the pore forms hydrogen bonds with the side chain of T237. All labeled residues are within 4 Å of BrEtOH molecules.

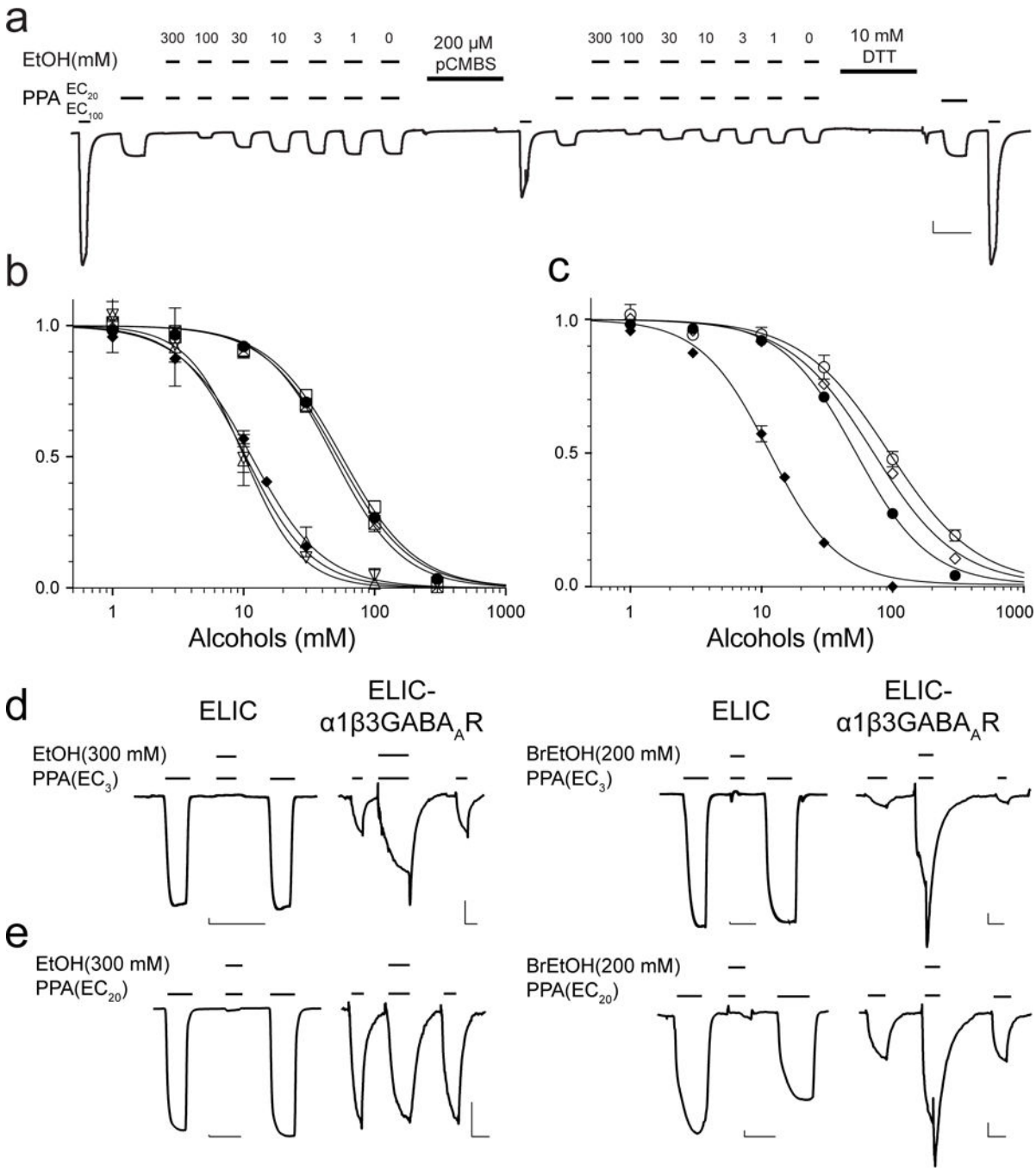

Figure 4. Alcohol binding to the pore determines functional inhibition of ELIC

(**a**) A representative trace of ethanol (EtOH) inhibition of the I23C/Y102F ELIC mutant, showing that labeling 4-chloromercuribenzenesulfonic acid (pCMBS) to I23C in the ECD binding pocket reduced the agonist-elicited current, but did not change EtOH modulation as quantified in (b). 10 mM DTT recovered the normal response to agonist activation by removing the pCMBS labeling. The vertical and horizontal scale bar represents 1 μA and 60 s, respectively. (**b**) Neither the ECD mutations nor pCMBS labeling affects the inhibition of ELIC by EtOH and 2-bromoethanol (BrEtOH). EtOH inhibition of ELIC (•, IC_{50} = 52.1

± 1.5 mM), I23C/Y102F in the absence of pCMBS labeling (⊠, IC_{50} = 48.6 ± 2.0 mM), and in the presence of pCMBS labeling (■, IC_{50} = 56.2 ± 2.5 mM); BrEtOH inhibition of ELIC (◆, IC_{50} = 11.5 ± 0.4 mM), I23C/Y102F in the absence of pCMBS labeling (▽, IC_{50} = 10.1 ± 0.8 mM), and in the presence of pCMBS labeling (△, IC_{50} = 10.4 ± 2.0 mM). (**c**) The TMD T237(6′)A mutation alters the channel response to both EtOH and BrEtOH. EtOH inhibition of ELIC (•) and T237(6′)A (○, IC_{50} = 93.4 ± 6.0 mM), BrEtOH inhibition of ELIC (◆) and the T237(6′)A (◇, IC_{50} = 70.9 ± 3.6 mM). The data were normalized to the current at EC_{20} in the absence of EtOH or BrEtOH and fit to the Hill equation (solid lines, n ≥ 6). (**d**) Representative traces obtained at a low agonist concentration (EC_3) showing EtOH (left traces) or BrEtOH (right traces) inhibition of ELIC and potentiation of ELIC-α1β3GABA$_A$R. (**e**) At EC_{20}, EtOH (left traces) or BrEtOH (right traces) strongly inhibit ELIC. EtOH shows no inhibition of ELIC-α1β3GABA$_A$R, while BrEtOH still shows some potentiation. The vertical and horizontal scale bars in (d, e) represent 30 nA and 60 s, respectively.

Table 1

Data collection and refinement statistics.

	ELIC-BrEtOH-PPA[a]	ELIC- BrEtOH[a]
Data collection		
Space group	$P2_1$	$P2_1$
Cell dimensions		
a, b, c (Å)	105.9, 266.8, 111.1	105.7, 266.9, 111.4
α, β, γ (°)	90, 107.1, 90	90, 106.9, 90
Wavelength (Å)	0.9195	0.9195
Resolution (Å)	39.61–3.10 (3.15–3.10)	39.63–3.40 (3.47–3.40)
Rpim (%)	3.1 (81.0)	7.2 (95.2)
R_{merge} (%)	18.4	46.7
$CC_{1/2}$	0.999 (0.600)	0.998 (0.424)
<I/σ>	19.0 (1.2)	12.2 (1.1)
No. reflections	3881779 (195188)	3480330 (167577)
Completeness (%)	99.9 (99.5)	99.9 (99.8)
Redundancy	36.5 (37.4)	43.1 (36.9)
Wilson B factors (Å^2)	115.9	104.3
Anomalous (Å)	5.5	6.3
Refinement		
Resolution (Å)	30 – 3.10	30 – 3.40
No. reflections	210329	159600
R_{work}	0.1996	0.2150
R_{free}	0.2387	0.2588
No. atoms		
Protein	25160	25160
Solvent	125	130
BrEtOH	128	128
PPA	40	–
B-factors (Å^2)		
Proteins	118.1	117.4
Solvent	152.2	146.6
BrEtOH	131.2	129.1
PPA	102.3	–
R.m.s deviations		
Bond lengths (Å)	0.006	0.003
Bond angles (°)	1.328	0.842
PDB code	5SXU	5SXV

[a] merged from 2 datasets with anomalous scaling.